BioMetals (2005) 18:375–386
DOI 10.1007/s10534-005-3712-z

Molecular dynamics simulations of the periplasmic ferric-hydroxamate binding protein FhuD

Karla D. Krewulak[1], Craig M. Shepherd[1,2] & Hans J. Vogel[1,*]
[1]*Structural Biology Research Group, Department of Biological Sciences, University of Calgary, 2500University Drive N.W, Calgary, Alberta, CanadaT2N 1N4;* [2]*The Scripps Research Institute, TPC-6 10550 N. Torrey Pines Road, La Jolla, CA, U.S.A.; *Author for correspondence (Tel: 403-220-6006; Fax: 403-289-9311; E-mail: vogel@ucalgary.ca)*

Key words: computer simulation, iron, molecular dynamics, periplasm, siderophore

Abstract

FhuD is a periplasmic binding protein (PBP) that, under iron-limiting conditions, transports various hydroxamate-type siderophores from the outer membrane receptor (FhuA) to the inner membrane ATP-binding cassette transporter (FhuBC). Unlike many other PBPs, FhuD possesses two independently folded domains that are connected by an α-helix rather than two or three central β-strands. Crystal structures of FhuD with and without bound gallichrome have provided some insight into the mechanism of siderophore binding as well as suggested a potential mechanism for FhuD binding to FhuB. Since the α-helix connecting the two domains imposes greater rigidity on the structure relative to the β-strands in other 'classical' PBPs, these structures reveal no large conformational change upon binding a hydroxamate-type siderophore. Therefore, it is difficult to explain how the inner membrane transporter FhuB can distinguish between ferrichrome-bound and ferrichrome-free FhuD. In the current study, we have employed a 30 ns molecular dynamics simulation of FhuD with its bound siderophore removed to explore the dynamic behavior of FhuD in the substrate-free state. The MD simulation suggests that FhuD is somewhat dynamic with a C-terminal domain closure of 6° upon release of its siderophore. This relatively large motion suggests differences that would allow FhuB to distinguish between ferrichrome-bound and ferrichrome-free FhuD.

Introduction

All bacteria have a need to acquire nutrients such as monosaccharides, oligosaccharides, amino acids, oligopeptides, oxyanions, cations, and vitamins from their environment. In Gram negative bacteria, acquisition of these nutrients requires passage across two membranes: the outer and the cytoplasmic membranes. Some of the nutrients (e.g. simple sugars, amino acids, and cations) are small enough to enter the periplasmic space by passive diffusion through the porins: trimeric outer membrane proteins that contain pores of a size that allows for the diffusion of nutrients that are less than 600 Da (Nikaido 2003). Other nutrients that are too large to pass through the porins (e.g. ferric-siderophores and vitamin B_{12}) rely on specialized outer membrane receptors for translocation into the periplasmic space (Braun & Braun 2002). The role of the PBPs is to scavenge nutrients in the periplasmic space and couple them to the inner membrane transporters for transport into the bacterial cytoplasm for subsequent use in a variety of bacterial cell processes.

While Gram-positive bacteria only have one membrane, they rely on similar membrane-anchored PBPs for the capture and transport of nutrients into the cytoplasm (Köster 2001). Numerous three-dimensional structures of PBPs have been solved by X-ray crystallography (for

reviews see Quiocho & Ledvina 1996; Fukami-Kobayashi *et al.* 1999; Krewulak *et al.* 2004). Although the amino acid sequence similarity between various PBPs is limited, most display a bilobal architecture in which the lobes are connected by two or three β-strands. Each lobe is independently folded and is composed of a mixed α/β structure. In most PBPs, these connecting β-strands form a region that allows the two lobes to twist with respect to each other and entrap the substrate in the cleft between the two domains. This 'Venus flytrap' or 'Pac Man' hinge motion is common amongst the PBPs where the two lobes are connected by β-strands. An example is the ferric ion binding protein from *Haemophilus influenzae*: FbpA. Comparison of the apo- and holo-FbpA structures reveal a 21° rotation of the two structural domains upon ferric ion binding (Bruns *et al.* 1997, 2001). Similar motions have been documented for the related maltose-binding protein (Spurlino *et al.* 1991; Shilton *et al.* 1996; Quiocho *et al.* 1997; Stockner *et al.*, submitted for publication), the nickel-binding protein (Heddle *et al.* 2003), and the glutamine-binding protein (Pang *et al.* 2003) for example.

One group of PBPs, however, behaves differently from the classical PBP. Here, the two independently folded lobes of the proteins PsaA, TroA, BtuF, and FhuD are connected by a long α-helix running along the backbone of the protein rather than β-strands (Figure 1). Because of the rigidity that this α-helix imposes on the overall protein structure, it is difficult to envisage how binding of the respective substrates could be accompanied by a large domain reorientation. Indeed only a small local change in the active site region was observed when comparing the crystallographic structures of the apo- and holo- vitamin-B_{12}-binding protein BtuF (Borths *et al.* 2002; Karpowich *et al.* 2003), the Zn^{2+}-binding protein TroA (Lee *et al.* 1999, 2002), and the ferrichrome-binding protein FhuD (Clarke *et al.* 2000; Krewulak *et al.*, submitted for publication). This outcome, however, left the question as to how the associated cytoplasmic transport proteins could distinguish between the ligand-bound and free proteins. Therefore, in an attempt to investigate the conformational space that is available to the siderophore-binding protein FhuD in the apo state, we have performed a molecular dynamics (MD) simulation of the protein. Herein, the results of this simulation will be discussed.

Materials and methods

Molecular dynamics simulation

Crystal structures are known for FhuD bound to gallichrome (1EFD) (Clarke *et al.* 2000) and various other hydroxamate-type siderophores (coprogen, desferal, and albomycin) which have the protein databank codes of 1ESZ, 1K2V, and 1K7S, respectively (Clarke *et al.* 2002). At the time that this study was initiated, the structure for apo-FhuD had not yet been reported, however it is now also available (Krewulak *et al.*, submitted for publication). The MD simulation described in this work was started from the high-resolution gallichrome-bound FhuD structure (1EFD) with the gallichrome and the crystallographic waters removed. Side chains missing from 1EFD (residues Glu86, Glu111, Arg115, Lys136, Val170, Lys171, and Arg186) were modeled using the program O (Jones *et al.* 1991). The most common sidechain conformation, as determined from the side chain library present in O, was chosen for each of these residues.

The simulations were performed with GROMACS v2.1 (Berendsen *et al.* 1995; Lindahl *et al.* 2001). FhuD was placed in the center of a rectangular box of approximate dimensions 86.91 × 75.36 × 92.24 Å. The system was solvated with simple point charge ('SPC') water, as previously described (Berendsen *et al.* 1981; Hermans *et al.* 1984). Additionally, 7 Na^+ atoms were introduced to compensate for the net negative charge on the protein. These ions were introduced by replacing the seven water molecules with the most favorable electrostatic potential. In total there were 57689 atoms in the simulation; 18355 of these were water molecules. Before the simulations were started, the system was energy minimized using the steepest descent method. Following energy minimization, the solvent (water and counter ions) was relaxed in a 500 picosecond simulation in which an isotropic force constant of 1000 kJ mol^{-1} nm^{-1} was imposed on all non-hydrogen protein atom positions. Constant temperature and pressure were maintained through weak coupling to an external bath (Berendsen *et al.* 1981) of 300 K and 1 bar using coupling constants of 0.1 and 0.5 ps, respectively. Electrostatics were calculated using Particle Mesh Ewald summation (Darden *et al.* 1993; Essmann *et al.*

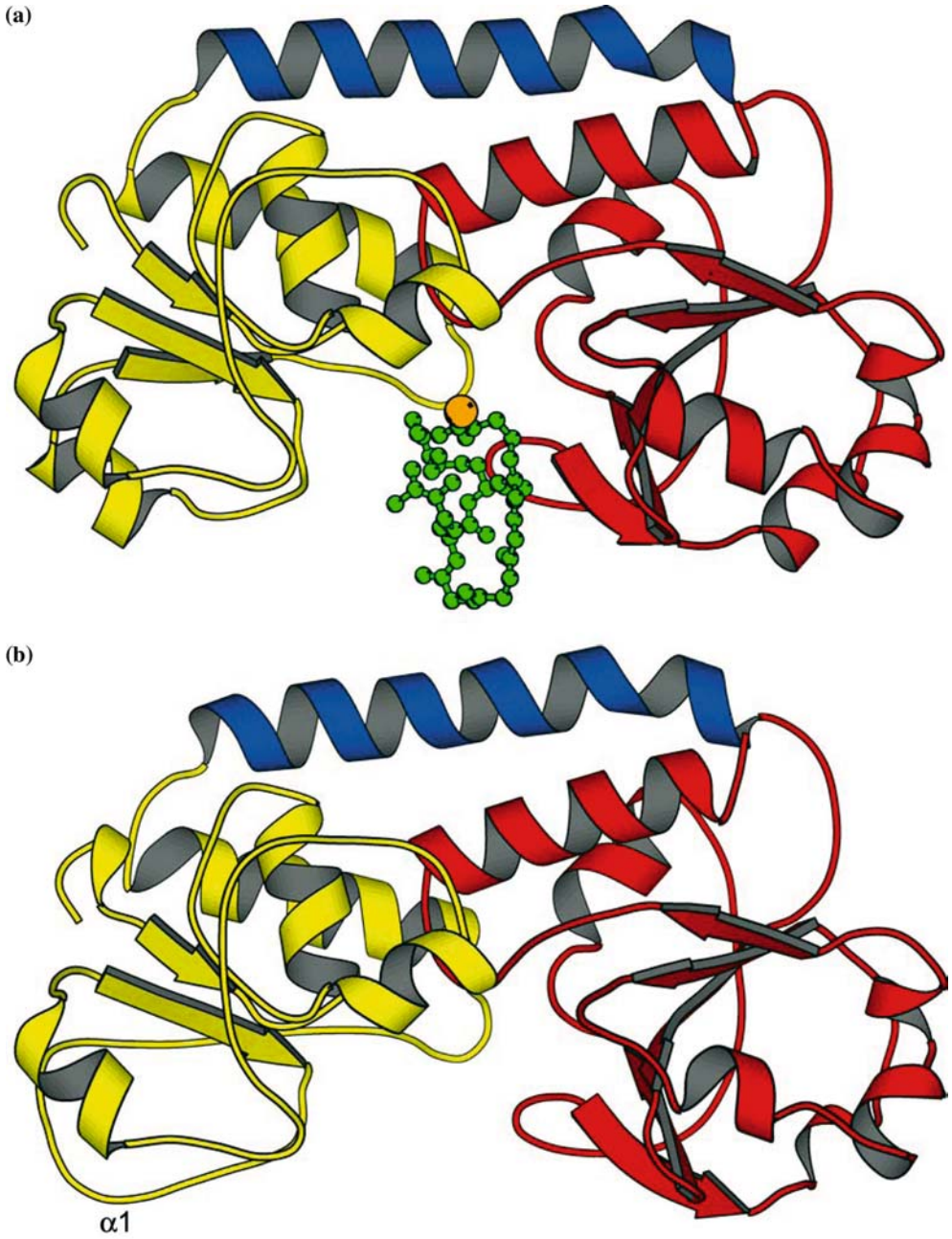

Figure 1. Ribbon representation of gallichrome-bound FhuD. A ribbon diagram of (a) gallichrome-bound and (b) gallichrome-free FhuD. The gallichrome-bound structure was solved using gallium for crystallographic phase information, but otherwise is identical to that of ferrichrome-bound FhuD. The N-terminal domain is colored yellow, the C-terminal domain is colored red, and the interdomain helix colored blue. Upon release of gallichrome, helix α1 unwinds.

1995) with a real-space cutoff of 10 Å and a Fourier spacing of 1.2 Å. Lennard–Jones interactions were truncated at 10 Å, and all non-bonded interactions were updated every 10 simulation steps. The total time of the simulation was 30 ns.

Analyses

Root mean square deviation (RMSD) and radius of gyration plots were generated using the analysis programs available in the Gromacs suite

(Berendsen *et al*. 1995; Lindahl *et al*. 2001). The Dyndom server was used to analyze the domain motions during the simulation (http://www.cmp.uea.ac.uk/dyndom/main.jsp) (Hayward & Lee 2002; Lee *et al*. 2003).

The radius of gyration for the crystal structures of various PBPs as well as for the final simulation structure for FhuD were calculated with the program Crysol (Svergun *et al*. 1995) using PDB files that were edited to remove multiple chains, water molecules, and with sidechains added where needed (Jones *et al*. 1991).

Sequence alignments

Sequence alignments were performed using sequences of the FhuD proteins from the Gram negative bacteria *E. coli*, *Salmonella typhimurium*, *Salmonella enterica*, *Shigella flexneri*, *Yersinia pestis*, *Vibrio mimicus*, and *Vibrio vulnificus* using the ClustalW server (Thompson *et al*. 1994).

Figures

All images were generated with Molmol (Koradi *et al*. 1996) or Molscript (Kraulis 1991), and rendered with Raster3D (Merritt & Bacon 1997).

Results

C-terminal domain motion

Evaluation of the change in the overall structure for the 30 ns simulation is provided by analysis of the C_α root mean square deviations (RMSD) relative to the initial structure as a function of time (Figure 2). An initial jump of 1 Å is seen within the first 0.1 ns of the simulation. This is typical of most simulations where the protein relaxes after being released from its more restrictive crystallographic environment. Other smaller increases in the RMSD are seen, most notably around 14 ns. The most mobile regions are pictorially represented in Figure 3 where the thickness of the lines is directly related to the mobility of that region throughout the simulation.

To fully characterize the differences in conformation that occurred in the simulation, FhuD was divided into the N-terminal domain (residues 32–145), the backbone α-helix (residues 146–171), and the C-terminal domain (residues 172–293). The N-terminal domain remains relatively static during the simulation with an RMSD of 1.57 Å between the starting structure and the final structure. The backbone α-helix also remains relatively static during the simulation with an RMSD of 1.75 Å

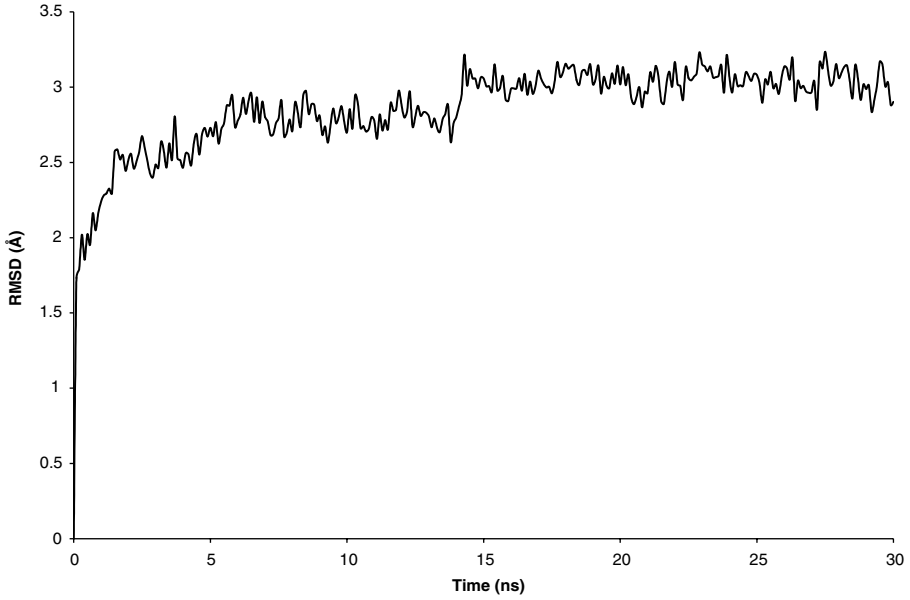

Figure 2. Root mean-square deviation of the backbone conformation of FhuD relative to the initial conformation at the start of the simulation. The RMSD relative to the starting (crystal) structure was calculated every 100 ps of the simulation using the suite of programs available from Gromacs (Berendsen *et al*. 1995; Lindahl *et al*. 2001).

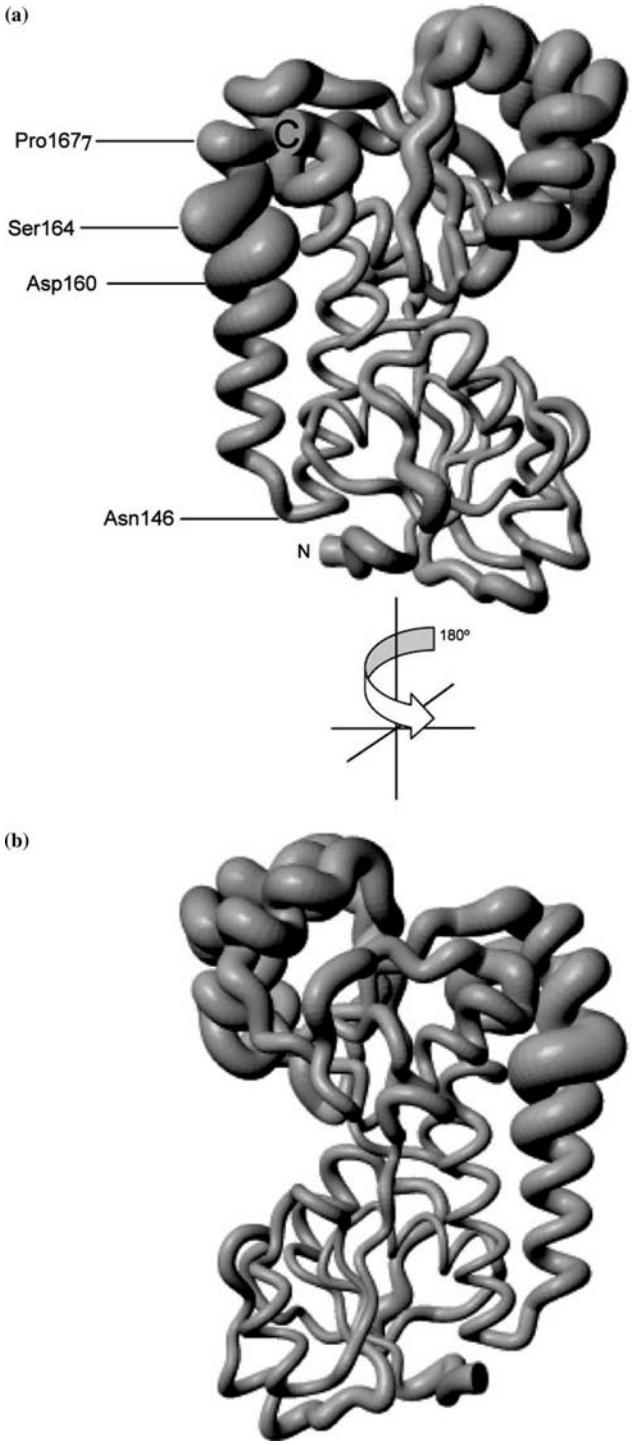

Figure 3. Sausage diagram demonstrating the range of motions observed during simulation trajectories. Every 10 ps of the FhuD MD simulation, a pdb file was written. The N-terminal domains (residues 32–145) of these files were overlayed in Molmol (Koradi *et al*. 1996) to make a sausage diagram. The thicker the line, the more mobile the region is throughout the simulation. The C-terminal domain is the most mobile with its motion originating from Asn146. The thickness of the line for the region Asp160 to Pro167 of the α-helix indicates it is mobile during the simulation; however, the α-helix retains its secondary structure throughout the entire course of the simulation.

between the starting and final structure. The rigidity of these structures throughout the simulation is further shown when the starting and final structure files for either the N-terminal domain or the α-helix are entered into the DynDom server and no dynamic domains are found. The C-terminal domain, however, appears to be somewhat more dynamic. Alignment between the starting and final structure gives a RMSD of 2.22 Å. Furthermore, when the starting and final structure files for the C-terminal domain of FhuD are entered into the DynDom server, a dynamic domain is found (Figure 4). The motion detected is a hinge rotation of 22.7° of two sets of residues (226–235 and 256–265; colored red in Figure 4) relative to the fixed domain (267–286; colored blue in Figure 4). When the N-terminal domains for the starting and final PDB structure files are aligned, a 6° closure of the C-terminal domain along an axis parallel to the α-helix is seen (Figure 5a). The same alignment with the crystallographically determined structures of holo and apo FhuD shows a 2° opening of the C-terminal domain (Figure 5b) (Krewulak *et al.*, submitted for publication). Looking at Figure 3, this motion appears to originate from the N-terminal portion of the backbone α-helix (Asn146).

Radius of gyration

In 1993, Tam and Saier analyzed the amino acid sequences of the PBPs that were available at the time from Gram negative bacteria and lipoproteins of Gram positive bacteria in an attempt to define the degree of relatedness between the PBPs (Tam & Saier Jr. 1993). This analysis produced eight different clusters of PBPs which somewhat correlated with molecular weight of the protein or the chemical nature of its bound ligand. Proteins that bind oligosaccharides, such as maltodextrin-binding protein (MBP), belong to cluster 1. Proteins that bind organic metal ion complexes include vitamin B_{12} binding protein (BtuF), and ferric siderophore complexes (FhuD, this study), belong to cluster 8. A new class, cluster 9, introduced more recently (Claverys 2001) includes proteins that bind zinc and manganese (TroA and PsaA, respectively) (Lawrence *et al.* 1998; Lee *et al.* 1999). Both Cluster 8 and 9 proteins consist of proteins that have an α-helix that spans the entire PBP.

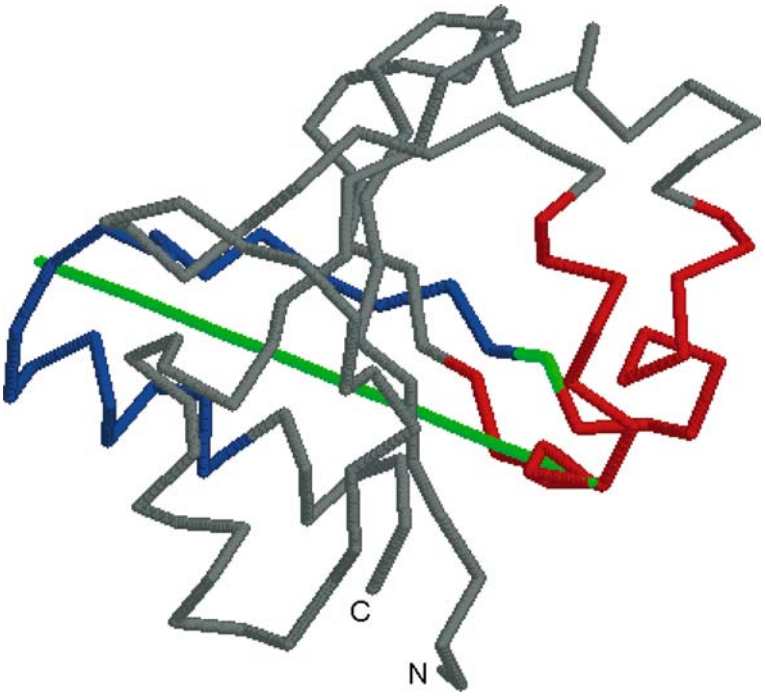

Figure 4. C-terminal domain tilting of FhuD observed during the MD simulation. The beginning and final structures from the C-terminal domain (172–293) of the apo-FhuD MD simulation were entered into the Dyndom server. The green residues represent the hinge domain. The blue residues represent the fixed sub-domain. The red residues represent the moving sub-domain.

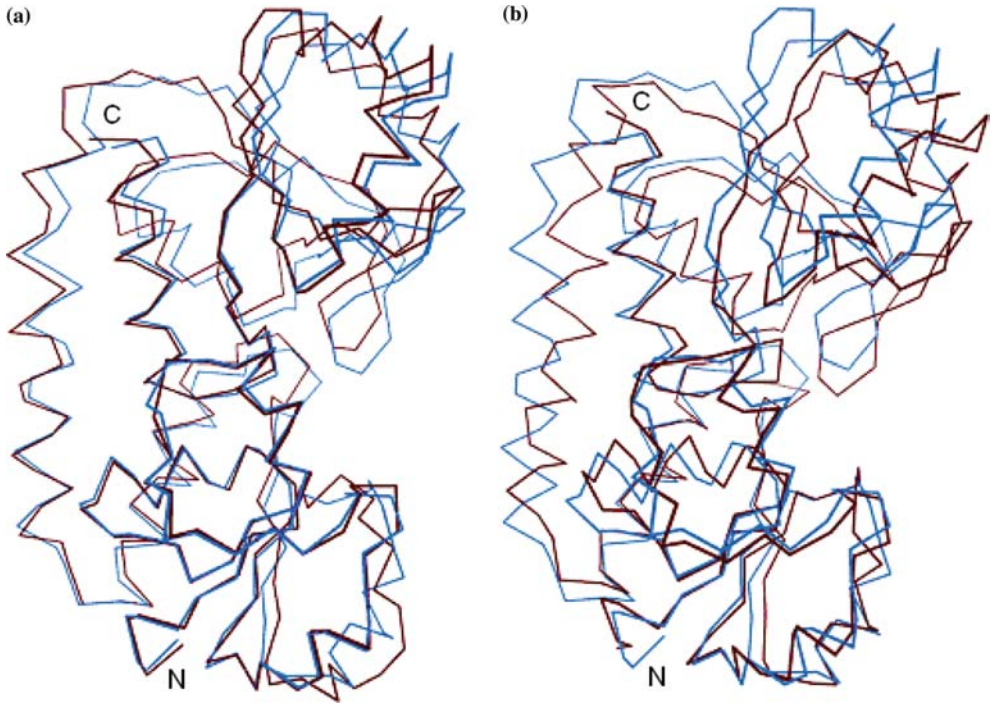

Figure 5. Superimposed C_α-backbone diagrams of apo-FhuD and ferrichrome-bound FhuD. The structures of ferrichrome-free (from the crystal structure (a) and the MD simulation (b) and ferrichrome-bound FhuD were superimposed by least-squares fit of residues 32–145; the N-terminal domain. The ferrichrome-bound and ferrichrome-free forms are colored red and blue, respectively. Note that the C-terminal domain of the crystal structure or apo-FhuD (a) opens via tilting of the C-terminal domain approximately 2° about an axis parallel to the backbone α-helix. The MD simulation of apo-FhuD shows closure of this C-terminal domain by approximately 6° about an axis parallel to the backbone α-helix. The N- and C-termini are labeled.

This α-helix probably prevents large hinge and twist motions often observed with other PBPs. For example, the best characterized PBP, MBP, rotates 35° along an axis parallel to its central *β*-strands upon ligand binding (Sharff *et al*. 1992). This large rotation results in a 6.6% reduction in radius of gyration (R_g) from 21.82 Å to 20.66 Å; calculated for the maltodextrin-free and bound forms, respectively. The apo and holo structures solved for the Cluster 8 proteins BtuF (Borths *et al*. 2002; Karpowich *et al*. 2003) and FhuD (Clarke *et al*. 2000; Krewulak *et al*., submitted for publication) and the Cluster 9 protein, TroA (Lee *et al*. 1999, 2002) show no large domain motion upon binding of their respective ligands. To compare the degree of domain reorganization upon ligand binding, the R_g value for FhuD was calculated relative to the initial structure as a function of time (Figure 6). Additionally, R_g values were calculated for proteins from various other clusters of PBPs (Table 1).

Discussion

We have carried out an MD simulation of the ferric-hydroxamate-binding protein FhuD. The MD simulation reveals a much larger domain motion than what was seen in the crystal structures of the ferrichrome-bound and free structures of FhuD. However, there are numerous differences identified between the apo-FhuD crystal structure and the MD simulation that can be attributed to the different environments of FhuD in the crystal structure versus the MD simulation.

The apo-FhuD structure was solved to 2.85 Å by X-ray crystallography (Krewulak *et al*., submitted for publication). The overall structure is almost identical to the crystal structure for gallichrome-bound FhuD except for the unwinding of helix α1 in the apo-protein (labeled in Figure 1). This helix unwinding is not found in the MD simulation, and may require a longer timescale. The apo-FhuD structure was solved with two

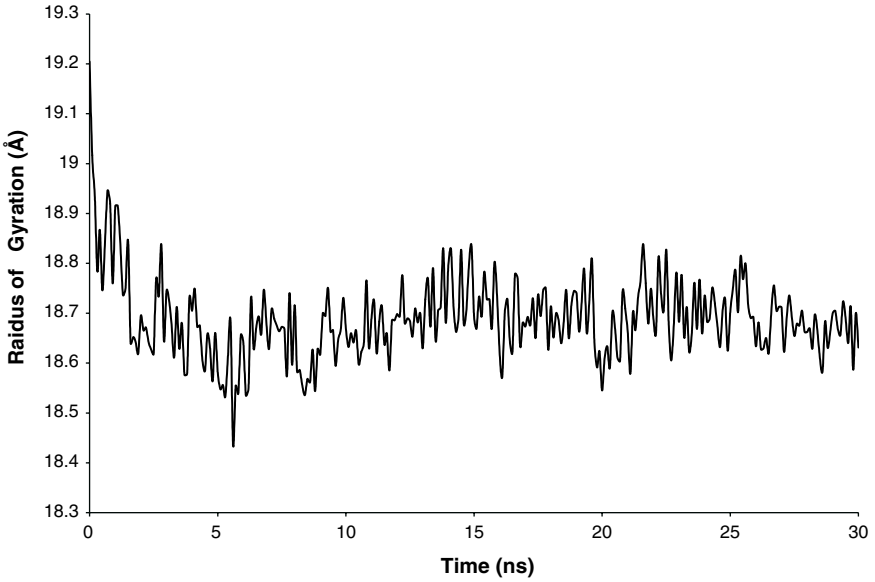

Figure 6. Radius of gyration (R_g) of all atoms relative to the initial conformation. The R_g was calculated every 100 ps of the simulation using the suite of programs available from Gromacs (Berendsen *et al*. 1995; Lindahl *et al*. 2001).

molecules per asymmetric unit in the hexagonal space group $P6_522$. Despite the high solvent content of protein crystals, a total of 24 molecules in the unit cell results in numerous interactions (e.g. hydrogen bonding) between symmetry related molecules thus greatly limiting the mobility of the individual FhuD molecules in the crystal. The only time when the reduced mobility of FhuD is comparable in the periplasm is when it is bound to FhuB. Similar to the vitamin B_{12}-binding protein BtuF, FhuD is thought to dock onto FhuB through interaction of the negatively charged Asp and Glu residues on the apices of the FhuD lobes with the positively charged Arg pockets on FhuB (Borths *et al*. 2002). Once FhuD is docked onto FhuB, a structural change must occur to reduce the affinity of FhuD for ferrichrome. Retraction of a loop adjacent to helix α1 accomplishes this by

Table 1. Ferric ion binding protein (FBP); maltodextrin-binding protein (MBP); Nickle-binding protein (NikA); Leucine isoleucine valine-binding protein (LIVBP); glucose/galactose-binding protein (GBP).

Protein	Cluster	Radius of gyration (Å)
FhuD (apo)	8	18.58
FhuD (holo)		19.15
BtuF (apo, chain A)	8	19.2
BtuF(holo, chain A)		18.8
TroA (apo)	9	18.87
TroA (holo)		19.21
FBP (apo)	1	19.9
FBP (holo)		19.14
MBP (apo)	1	21.82
MBP (holo)		20.66
NikA (apo, chain A)	5	24.3
NikA (holo, chain A)		23.9
LIVBP (apo)	4	22.2
LIVBP (holo, Leu bound)		23.3
GBP (apo)	1	21.81
GBP (holo)		20.3

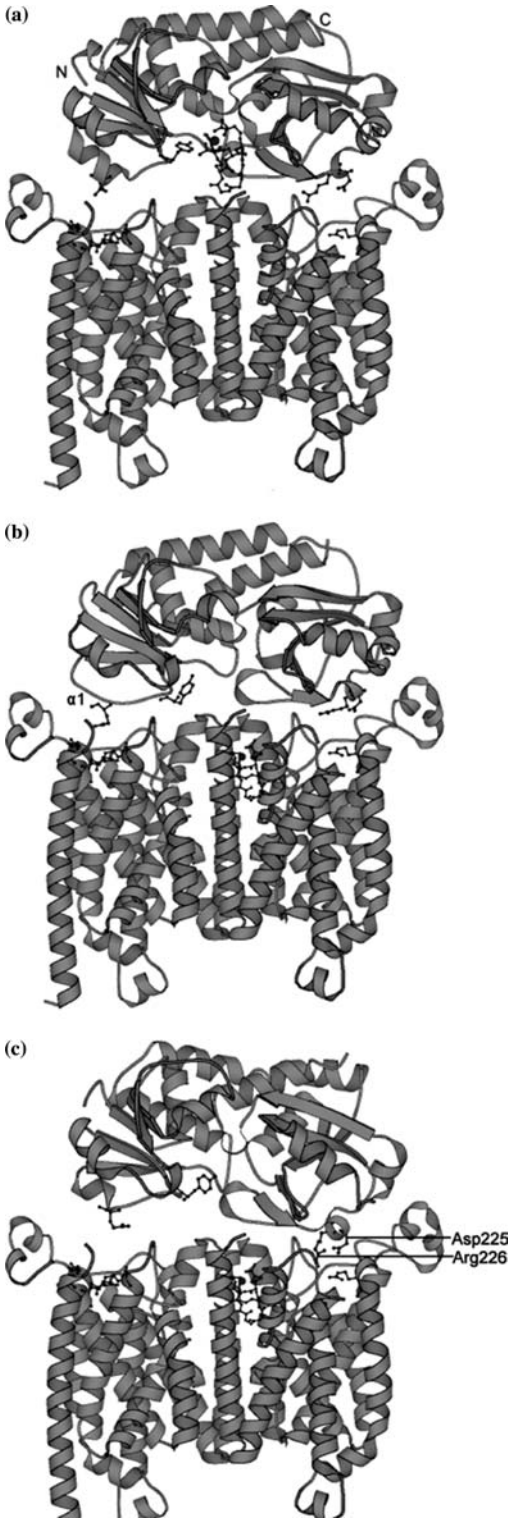

Figure 7. Possible docking of FhuD onto FhuB. FhuD bound to ferrichrome (a, top ribbon structure) interacts with FhuB (a, bottom ribbon structure). The sidechains of residues Glu111 and Asp225 from FhuD (shown in ball-and-stick representation) form salt bridges with the Arg residues (ball-and-sticks) of FhuB. The active site residue that locks ferrichrome in place (Tyr106) is also shown in ball-and-stick representation. Once bound, the helix adjacent to Tyr106 unwinds ultimately resulting in retraction of Tyr106 and subsequent release of ferrichrome to FhuB (b). Dissolution of the salt bridge occurs upon C-terminal domain tilting of FhuD (c). FhuD is now released into the periplasm to acquire additional ferric hydroxamate-type siderophores for transport into the bacterial cytoplasm.

removing the interaction of ferrichrome with Tyr106, a residue that is of crucial importance for ferrichrome binding as shown by site directed mutagenesis (data not shown). Once Tyr106 is retracted, the binding pocket is now less favorable and can release ferrichrome to the FhuB cavity (Figure 7). Additional to retraction of this loop, the helix α1 unwinds. This displaces Glu111, a residue that tethers the N-terminal domain of FhuD to FhuB through formation of a salt bridge with one of the two Arg rich pockets of FhuB. This unwinding could possibly facilitate the release of the now ferrichrome-free FhuD to bind another ferrichrome molecule.

The conditions of the MD simulation more closely resemble the environment FhuD experiences when it is freely moving in the periplasm. Now that there are no longer interactions between adjacent molecules, as seen in the crystal, a greater range of movement is identified with the MD simulations of FhuD. This includes the dynamic reorganization of the C-terminal domain. As discussed in the previous paragraph, ferrichrome has been released to FhuB after the retraction of the loop containing Tyr106 (Figure 7b). Additionally, the N-terminal domain of FhuD has been released from FhuB by the unwinding of helix α1. The 6° closure of the C-terminal domain seen in the MD simulation would tilt Glu111 further from one of the Arg-rich pockets of FhuB as well as result in the movement of the positively charged residue, Arg226, towards the Arg-rich pocket of FhuB (Figure 7c). This creates charge repulsion and would facilitate the release of the C-terminal domain of FhuD from FhuB. With both domains released, FhuD is ready to bind another ferrichrome molecule. It is interesting to note that,

upon examination of a sequence alignment of FhuDs from various Gram negative bacteria, it is found that the Arg226 residue is highly conserved (Figure 8). The possible role of this conserved residue has not been addressed until now.

Because transport of ferrichrome requires ATP hydrolysis by the inner membrane transporter (FhuBC), FhuBC must be able to distinguish between ferrichrome bound and free FhuD in order to be energetically efficient. Until now, it was unknown how the FhuBC transporter recognizes ferrichrome-bound versus the ferrichrome-free FhuD. The crystal structures of apo and vitamin-B_{12} BtuF and apo- and ferrichrome-bound FhuD reveal such a small structural change that the distance between the negatively charged Asp and Glu residues does not differ significantly from the ligand-bound structures. The distances between the CD atom of Glu111 and the CG atom of Asp225 for the ferrichrome bound and ferrichrome-free FhuD crystal structures are 41.5 Å, and 43.3 Å, respectively. The distances between the Arg-rich pockets of FhuB (as measured by the distance between the CZ atoms of Arg61 and Arg393) is 41.5 Å. Taking into account the conformational flexibility of Arg residues, this suggests that the crystallographically determined apo forms of these two proteins could still interact with the negatively charged residues of the transporter. A distance of 35.8 Å was measured between the CG atom of Asp225 and atom CD of Glu111 at the end of the MD simulation. Therefore, when there is no ferrichrome (or another hydroxamate-type siderophore) bound to FhuD, the distance between the negatively charged residues is reduced thereby breaking the interactions between FhuD and FhuB. Such a mechanism would explain how FhuB can distinguish between ferrichrome-bound and ferrichrome-free FhuD. This further suggests that cluster 8 and 9 proteins are more dynamic than the crystallographic structures suggest.

Conclusions

The overall architectures of close to 100 different PBPs have been reported in the protein databank to date. Presently, the mechanism for binding (and release) of FhuD to FhuB is not well understood. Crystallographic studies would help to support the

Figure 8. Sequence alignment of FhuD proteins from *S. typhimurium*, *S. enterica*, *E. coli*, *S. flexneri*, *Y. pestis*, *V. mimicus*, and *V. vulnificus* done on Clustal-W server (Thompson *et al.* 1994). The conserved Glu and Asp residues that are important for FhuD binding to FhuB are indicated by boxes. Additionally, a conserved Arg (or Lys) residue that may play a role in the release of FhuD from FhuB is indicated by a box.

hypothesis that, to transport siderophores to the cytoplasm, the negatively charged residues on the apices of FhuD interact with the positively charged pockets on the periplasmic face of FhuB. Transport studies coupled with site directed mutagenesis are currently being utilized to understand which of the negatively charged residues are most important for transport of ferrichrome. This could be accompanied by MD simulations similar to what Gruia *et al.* performed on the enzyme Staphylococcal nuclease to understand the kinetics of breaking an Arg–Glu salt bridge (Gruia *et al.* 2003). Because the structures of the PBP (BtuF) and the inner membrane ABC transporter structure (BtuCD) have been solved (Locher *et al.* 2002), its coordinates could be used in these MD studies along with steered MD to understand what conformational changes are relevant for the transport of siderophores into the cytoplasm (Oloo & Tieleman 2004). The evolutionary relatedness between the different clusters of PBPs allows for any information derived from these MD simulations to be applied to the FhuD pathway as well as all other related PBPs.

Acknowledgements

This work was supported by an operating grant from the Canadian Institute for Health Research (CIHR) to H.J.V. H.J.V. holds a Medical Scientist Award from the Alberta Heritage Foundation for Medical Research (AHFMR). K.D.K is the holder of postgraduate awards from the Natural Sciences and Engineering Research Council of Canada (NSERC) and AHFMR. We appreciate various discussions on this topic with Drs. T. Stockner, C. Kandt, and P. Tieleman.

References

Berendsen HJC, Postma JPM, Van Gunsteren WF, Hermans J. 1981 Interaction models for water in relation to protein hydration. In: Pullman B, (Ed.). *Intermolecular Forces*. D. Reidel Publishing Company;Dordrecht: pp. 331–342.

Berendsen HJC, VanderSpoel D, VanDrunen R. 1995 Gromacs – A Message-Passing Parallel Molecular-Dynamics Implementation. *Comput Phys Commun* **91**, 43–56.

Borths EL, Locher KP, Lee AT, Rees DC. 2002 The structure of *Escherichia coli* BtuF and binding to its cognate ATP binding cassette transporter. *Proc Natl Acad Sci USA* **99**, 16642–16647.

Braun V, Braun M. 2002 Iron transport and signaling in *Escherichia coli*. *FEBS Lett* **529**, 78–85.

Bruns CM, Anderson DS, Vaughan KG, *et al.* 2001 Crystallographic and biochemical analyses of the metal-free *Haemophilus influenzae* Fe^{3+} -binding protein. *Biochemistry* **40**, 15631–15637.

Bruns CM, Nowalk AJ, Arvai AS, *et al.* 1997 Structure of *Haemophilus influenzae* Fe^{+3} -binding protein reveals convergent evolution within a superfamily. *Nat Struct Biol* **4**, 919–924.

Clarke TE, Braun V, Winkelmann G, Tari LW, Vogel HJ. 2002 X-ray crystallographic structures of the *Escherichia coli* periplasmic protein FhuD bound to hydroxamate-type siderophores and the antibiotic albomycin. *J Biol Chem* **277**, 13966–13972.

Clarke TE, Ku SY, Dougan DR, Vogel HJ, Tari LW. 2000 The structure of the ferric siderophore binding protein FhuD complexed with gallichrome. *Nat Struct Biol* **7**, 287–291.

Claverys JP. 2001 A new family of high-affinity ABC manganese and zinc permeases. *Res Microbiol* **152**, 231–243.

Darden T, York D, Pedersen L. 1993 Particle mesh Ewald – an N.Log(N) method for Ewald sums in large systems. *J Chem Phys* **98**, 10089–10092.

Essmann U, Perera L, Berkowitz ML, Darden T, Lee H, Pedersen LG. 1995 A smooth particle mesh Ewald method. *J Chem Phys* **103**, 8577–8593.

Fukami-Kobayashi K, Tateno Y, Nishikawa K. 1999 Domain dislocation: a change of core structure in periplasmic binding proteins in their evolutionary history. *J Mol Biol* **286**, 279–290.

Gruia AD, Fischer S, Smith JC. 2003 Molecular dynamics simulation reveals a surface salt bridge forming a kinetic trap in unfolding of truncated Staphylococcal nuclease. *Proteins* **50**, 507–515.

Hayward S, Lee RA. 2002 Improvements in the analysis of domain motions in proteins from conformational change: DynDom version 1.50. *J Mol Graphics Modell* **21**, 181–183.

Heddle J, Scott DJ, Unzai S, Park SY, Tame JR. 2003 Crystal structures of the liganded and unliganded nickel-binding protein NikA from *Escherichia coli*. *J Biol Chem* **278**, 50322–50329.

Hermans J, Berendsen HJC, Van Gunsteren WF, Postma JPM. 1984 A consistent empirical potential for water–protein interactions. *Biopolymers* **23**, 1513–1518.

Jones TA, Zou JY, Cowan SW, Kjeldgaard M. 1991 Improved methods for building protein models in electron-density maps and the location of errors in these models. *Acta Crystallogr A* **47**, 110–119.

Karpowich NK, Huang HH, Smith PC, Hunt JF. 2003 Crystal structures of the BtuF periplasmic-binding protein for vitamin B_{12} suggest a functionally important reduction in protein mobility upon ligand binding. *J Biol Chem* **278**, 8429–8434.

Koradi R, Billeter M, Wuthrich K. 1996 MOLMOL: a program for display and analysis of macromolecular structures. *J Mol Graph* **14**, 51–32.

Köster W. 2001 ABC transporter-mediated uptake of iron, siderophores, heme and vitamin B_{12}. *Res Microbiol* **152**, 291–301.

Kraulis PJ. 1991 Molscript – a program to produce both detailed and schematic plots of protein structures. *J Appl Crystallogr* **24**, 946–950.

Krewulak KD, Peacock RS, Vogel HJ. 2004 Periplasmic binding proteins involved in bacterial iron uptake. In: Crosa

JH, Mey AR, Payne SM, eds. *Iron Transport in Bacteria*. ASM Press Washington;Washington: pp. 113–129.

Lawrence MC, Pilling PA, Epa VC, Berry AM, Ogunniyi AD, Paton JC. 1998 The crystal structure of pneumococcal surface antigen PsaA reveals a metal-binding site and a novel structure for a putative ABC-type binding protein. *Structure* **6**, 1553–1561.

Lee RA, Razaz M, Hayward S. 2003 The DynDom database of protein domain motions. *Bioinformatics* **19**, 1290–1291.

Lee YH, Deka RK, Norgard MV, Radolf JD, Hasemann CA. 1999 *Treponema pallidum* TroA is a periplasmic zinc-binding protein with a helical backbone. *Nat Struct Biol* **6**, 628–633.

Lee YH, Dorwart MR, Hazlett KRO, *et al*. 2002 The crystal structure of Zn(II)-free *Treponema pallidum* TroA, a periplasmic metal-binding protein, reveals a closed conformation. *J Bacteriol* **184**, 2300–2304.

Lindahl E, Hess B, Spoel Dvan der. 2001 GROMACS 3.0: a package for molecular simulation and trajectory analysis. *J Mol Modell* **7**, 306–317.

Locher KP, Lee AT, Rees DC. 2002 The *E-coli* BtuCD structure: a framework for ABC transporter architecture and mechanism. *Science* **296**, 1091–1098.

Merritt EA, Bacon DJ. 1997 Raster3D: photorealistic molecular graphics. *Methods Enzymol* **277**, 505–524.

Nikaido H. 2003 Molecular basis of bacterial outer membrane permeability revisited. *Microbiol Mol Biol Rev* **67**, 593–656.

Oloo EO, Tieleman DP. 2004 Conformational transitions induced by the binding of MgATP to the vitamin B_{12} ATP-binding cassette (ABC) transporter BtuCD. *J Biol Chem* **279**, 45013–45019.

Pang A, Arinaminpathy Y, Sansom MS, Biggin PC. 2003 Interdomain dynamics and ligand binding: molecular dynamics simulations of glutamine binding protein. *FEBS Lett* **550**, 168–174.

Quiocho FA, Ledvina PS. 1996 Atomic structure and specificity of bacterial periplasmic receptors for active transport and chemotaxis: variation of common themes. *Mol Microbiol* **20**, 17–25.

Quiocho FA, Spurlino JC, Rodseth LE. 1997 Extensive features of tight oligosaccharide binding revealed in high-resolution structures of the maltodextrin transport chemosensory receptor. *Structure* **5**, 997–1015.

Sharff AJ, Rodseth LE, Spurlino JC, Quiocho FA. 1992 Crystallographic evidence of a large ligand-induced hinge-twist motion between the two domains of the maltodextrin binding protein involved in active transport and chemotaxis. *Biochemistry* **31**, 10657–10663.

Shilton BH, Flocco MM, Nilsson M, Mowbray SL. 1996 Conformational changes of three periplasmic receptors for bacterial chemotaxis and transport: the maltose-, glucose/galactose- and ribose-binding proteins. *J Mol Biol* **264**, 350–363.

Spurlino JC, Lu GY, Quiocho FA. 1991 The 2.3-Å resolution structure of the maltose-binding or maltodextrin-binding protein, a primary receptor of bacterial active-transport and chemotaxis. *J Biol Chem* **266**, 5202–5219.

Svergun D, Barberato C, Koch MHJ. 1995 CRYSOL – a program to evaluate X-ray solution scattering of biological macromolecules from atomic coordinates. *J Appl Crystallogr* **28**, 768–773.

Tam R, Saier MH Jr. 1993 Structural, functional, and evolutionary relationships among extracellular solute-binding receptors of bacteria. *Microbiol Rev* **57**, 320–346.

Thompson JD, Higgins DG, Gibson TJ. 1994 Clustal-W – Improving the sensitivity of progressive multiple sequence alignment through sequence weighting, position-specific gap penalties and weight matrix choice. *Nucleic Acids Res* **22**, 4673–4680.